Heart and Vessels (2019) 34:393–400
https://doi.org/10.1007/s00380-018-1255-9

ORIGINAL ARTICLE

Microbubble contrast enhancement of neointima after drug-eluting stent implantation: an optical coherence tomography study

Norikiyo Oka[1] · Tadayuki Kadohira[1] · Kenichi Fujii[1] · Hideki Kitahara[1] · Yoshihide Fujimoto[1] · Yoshio Kobayashi[1]

Received: 17 April 2018 / Accepted: 31 August 2018 / Published online: 5 September 2018

Abstract

Microvessels within neoatherosclerosis are associated with vulnerability and increase from the early to the very late phase after drug-eluting stent implantation. Microbubble contrast agents have been suggested to enhance tissue microvasculature for optical coherence tomography (OCT) imaging. The present study investigated whether OCT signal intensity of neointima within stented segments was enhanced after intracoronary administration of microbubble contrast agents. A total of 40 patients who underwent follow-up coronary angiography after drug-eluting stent implantation were enrolled. At the time of follow-up coronary angiography, OCT images of the stented segments were recorded before and after intracoronary administration of microbubble contrast agents. Mean OCT signal intensity of neointima after microbubble administration significantly increased [95.5 (85.7, 106.2) vs. 96.5 (88.7, 109.9), $p = 0.001$]. Multivariate analysis demonstrated the relationship between diabetes and greater neointima enhancement. The change in the OCT signal intensity of neointima following microbubble administration tended to be higher in diabetic patients than in non-diabetic patients [4.6 (0.6, 8.5) vs. 1.4 (−1.1, 3.0), $p = 0.05$]. These findings suggest that this methodology may allow identification of neovascularization in neointima and evaluation of vulnerability of neoatherosclerosis. Microvessels in neointima may be a future target of pharmacological and interventional innovations for preventing stent failure.

Keywords Neointima · Neoatherosclerosis · Microvessel · Optical coherence tomography · Microbubble

Abbreviations

CSA	Cross-sectional area
IQR	Interquartile range
OCT	Optical coherence tomography
NIH	Neointimal hyperplasia

Introduction

Coronary plaque neovascularization and subsequent intraplaque hemorrhage are associated with plaque vulnerability. In-stent neoatherosclerosis is an important substrate for late stent failure, including late/very late stent thrombosis and in-stent restenosis [1]. It is histologically characterized by an accumulation of lipid-laden foamy macrophages with or without necrotic core formation and/or calcification within neointima [2]. Previous pathological studies have reported that the incidence of in-stent neoatherosclerosis increased with time and that microvessels within in-stent neoatherosclerosis also increased from the early to the very late phase after drug-eluting stent implantation [2–4].

Optical coherence tomography (OCT) is considered feasible for the detection of microvessels due to its high resolution [4–6]. However, even with OCT, it is impossible to detect coronary plaque neovascularization that induces subsequent hemorrhage. Microbubble contrast-enhanced ultrasound has been used to detect carotid plaque neovascularization [7, 8]. Recently, microbubble contrast agents have been shown to be useful to enhance tissue microvasculature in OCT imaging [9–11]. It may be possible to detect coronary plaque neovascularization using microbubble contrast-enhanced OCT. The present study investigated changes in OCT signal intensity of neointima after intracoronary administration of microbubble contrast agents and evaluated clinical factors that were associated with the degree of signal intensity changes.

✉ Norikiyo Oka
norikiyo.oka@ma.point.ne.jp

[1] Department of Cardiovascular Medicine, Chiba University Graduate School of Medicine, 1-8-1 Inohana, Chuo-ku, Chiba, Chiba 260-8677, Japan

Materials and methods

Study design and population

The present study was a single center, prospective, non-randomized study. Routine follow-up coronary angiography 9 months after intravascular ultrasound-guided drug-eluting stent implantation [12] is performed at Chiba University Hospital. All patients who underwent 9-month follow-up coronary angiography after drug-eluting stent implantation were screened from August 2012 to December 2014. Exclusion criteria were (1) estimated glomerular filtration rate < 50 ml/min/1.73 m^2, (2) left ventricular ejection fraction < 30% or NYHA class III or IV, (3) ostial lesion of the left or right coronary artery, (4) patients treated with at least 1 bare metal stent at the index percutaneous coronary intervention, and (5) patients who were enrolled in another investigational trial. A total of 47 patients were enrolled. Of these, 7 patients were excluded due to the following reasons: poor OCT images ($n = 5$), unsuccessful guidewire passage ($n = 1$), and withdrawal of consent ($n = 1$). Finally, 40 patients were eligible for the final analysis. Clinical characteristics and settings of each participant were collected, and the definitions of each term were as follows. Hypertension was defined as blood pressure ≥ 140/90 mmHg, or taking antihypertensive drug at index PCI hospitalization. Diabetes mellitus was defined as fasting blood glucose ≥ 126 mg/dl or hemoglobin A_{1c} ≥ 6.5%, or taking diabetes treatment at index PCI hospitalization. Dyslipidemia was defined as fasting blood low-density lipoprotein cholesterol ≥ 140 mg/dl or fasting blood high-density lipoprotein < 40 or fasting blood triglyceride ≥ 150 mg/dl. The status of each drug use was recorded at the time of index PCI and follow-up coronary angiography.

This study was approved by the Chiba university ethical committee and was conducted in accordance with the Declaration of Helsinki. Written informed consent was obtained from all participants.

OCT image acquisition

Optical coherence tomography imaging was performed after routine follow-up coronary angiography. Immediately after intracoronary isosorbide dinitrate administration, an OCT catheter (Dragonfly JP, St Jude Medical, St. Paul, MN, USA) was introduced distal to the stented lesion, and contrast media were injected via the guiding catheter during pull back. An ILUMIEN OPTIS OCT imaging system (St. Jude Medical) was used for OCT image acquisition at 180 frames/s at a pullback speed of 18 mm/s. Sonazoid (Daiichi-Sankyo, Tokyo, Japan) consists of microbubbles that are micrometer-sized perflubutane gas spheres stabilized by a membrane of hydrogenated egg phosphate serine with a 2–3-μm diameter. The 2nd OCT imaging was performed 5 s after intracoronary administration of 2 ml of Sonazoid. OCT images were digitally stored for offline analysis.

Conventional OCT analysis

All analyses were performed by an experienced cardiologist using an off-line proprietary analysis program (St. Jude Medical) according to previous consensus standards and reports [13–15]. Quantitative OCT measurements were done for all available slices including the stented segment and 5-mm-long proximal and distal references. Stent cross-sectional area (CSA) and lumen CSA were manually measured at 1.0-mm intervals. Inadequate images including poor quality images and cross sections with major branches (> 90° of vessel wall or diameter > 2.0 mm) were excluded. Neointimal hyperplasia (NIH) CSA was calculated as the stent CSA minus the lumen CSA. The percent NIH CSA was defined as the NIH CSA divided by the stent CSA. NIH thickness was defined as the distance between the luminal surface of neointima and the strut. Microchannels were defined as signal-poor tubuloluminal structures located within neointima that were recognized on 3 consecutive cross-sectional images.

OCT signal intensity analysis

Neointima and microchannels were manually contoured on OCT images (Fig. 1a). Since it was difficult to visually recognize OCT signal intensity change, we utilized ImageJ software (National Institute of Health, Bethesda, MD, USA) to quantify OCT signal intensity. OCT signal intensity within the region of interest (ROI) at the frame level was calculated as the sum of OCT signal intensity per pixel within the ROI divided by the number of pixels within the ROI. OCT signal intensity within each ROI at the frame level was analyzed at 1.0-mm intervals for neointima, and at 0.1-mm intervals for microchannels. At the patient level, mean OCT signal intensity was calculated as the average of all the OCT signal intensities within each ROI at the frame level. OCT signal intensity change was calculated as the mean OCT signal intensity after microbubble administration minus that before microbubble administration. Measurement of OCT signal intensity in 10 randomly selected participants by 2 observers and by 1 observer at 2 separate sessions showed an interobserver correlation coefficient of 0.966 and an intraobserver coefficient of 0.998.

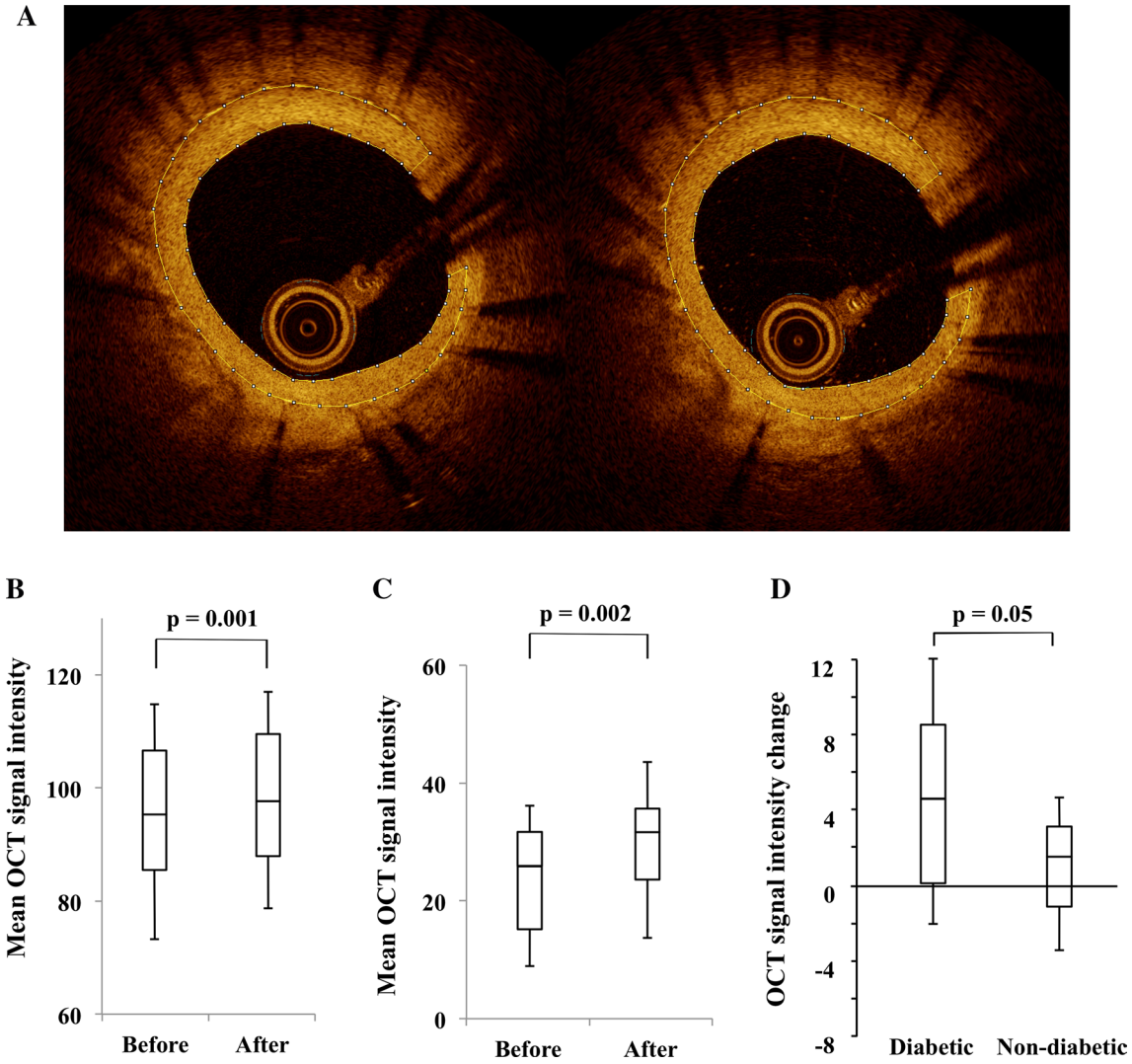

Fig. 1 **a** Representative optical coherence tomography images of neointima before and after intracoronary administration of microbubble contrast agents. Neointima of stented segments were manually contoured using ImageJ software (yellow lines). Left and right images showed example of frame before and after intracoronary administration of microbubble contrast agents. Optical coherence tomography (OCT) signal intensity was 105.0 and 113.3, respectively. OCT signal intensity per pixel within the region was analyzed at 1.0-mm intervals for neointima, and at 0.1-mm intervals for microchannels. At the patient level, mean OCT signal intensity was calculated as the average of all the OCT signal intensities within each ROI at the frame level. In this case, mean OCT signal intensity of neointima increased after intracoronary administration of microbubble contrast agents. **b**. Optical coherence tomography signal intensity of neointima before and after microbubble contrast administration. Note increase of optical coherence tomography signal intensity of neointima after microbubble administration. **c** Optical coherence tomography signal intensity of microchannels within neointima before and after microbubble contrast administration. Note increase in optical coherence tomography signal intensity of microchannels after microbubble administration. **d** Optical coherence tomography signal intensity change of neointima in diabetic and non-diabetic patients. Note higher change in optical coherence tomography signal intensity of neointima in diabetic patients

Statistical analysis

Categorical variables were presented as counts and percentages and compared using Chi-square tests or Fisher's exact tests as appropriate. Continuous variables were presented as median [interquartile range (IQR)] and compared using Mann–Whitney *U* test. Comparisons of OCT signal intensity before and after microbubble administration were performed using Wilcoxon's signed rank test. To evaluate clinical factors related to Δintensity of neointima (defined as the intensity increase after microbubble administration), Δintensity = 5 was set as the cutoff value. To identify predictors of Δintensity of neointima < 5, multivariate logistic regression analyses were used. Univariate variables with $p < 0.20$, and variables clinically supposed to be related to neoatherosclerosis were entered into the multivariate logistic models. All statistical analyses

were performed using SPSS version 23.0 software (SPSS Inc., Chicago, IL, USA). Two-sided p values <0.05 were considered statistically significant.

Results

Patients and procedural characteristics

Patient and procedural characteristics are presented in Table 1. Follow-up coronary angiography was performed at a median of 387.5 days (IQR 317.8–487.5).

OCT findings

OCT analysis showed a homogeneous pattern and no lipid, macrophage, or calcium in the neointima area of each stent. The mean NIH CSA and thickness were 1.1 (0.8, 1.4) mm^2 and 112.1 (90.3, 153.0) μm, respectively (Table 2). The percentage of cross sections with microchannels was 3.0 (1.6, 7.2)%. Mean OCT signal intensity of neointima significantly increased after microbubble administration [95.5 (85.7, 106.2) vs. 96.5 (88.7, 109.9), $p=0.001$] (Fig. 1b). There was a significant increase in mean OCT signal intensity in microchannels following administration of microbubble [27.4 (17.5, 32.0) vs. 32.5 (25.3, 35.0), $p=0.002$] (Fig. 1c).

Clinical factor relative to greater intensity increase

Logistic regression analysis demonstrated diabetes mellitus as a significant factor of greater intensity increase (Table 3). None of the other risk factors, including hypertension, dyslipidemia, smoking, and family history of coronary artery disease, were associated with OCT signal intensity increase of neointima after microbubble administration. Tables 4 and 5 show patient and procedural characteristics and OCT findings that are divided into 2 groups according to diabetic or non-diabetic patients. The difference in mean OCT signal intensities neither before nor after microbubble administration was significant between diabetic and non-diabetic patients. Baseline mean OCT signal intensity measured before microbubble administration was similar between diabetic patients and non-diabetic patients [98.6 (80.3, 106.1) vs. 94.6 (83.2, 113.3), $p=0.66$]. However, the change in OCT signal intensity of neointima by administration of microbubble tended to be higher in diabetic patients than in non-diabetic patients [4.6 (0.6, 8.5) vs. 1.4 (−1.1, 3.0), $p=0.05$] (Fig. 1d).

Discussion

The present study demonstrated that intracoronary administration of microbubble contrast agents enhanced OCT signal intensity of neointima area of the stent. In addition, the

Table 1 Patient and procedural characteristics

Variable	Overall ($n=40$)
Age (years)	70.0 (61.0, 77.0)
Men	30 (75.0)
Body Mass Index (kg/m^2)	22.8 (21.5, 25.1)
Current smoker	6 (15.0)
Hypertension	31 (77.5)
Diabetes mellitus	18 (45.0)
Insulin treated	2 (5.0)
Dyslipidemia	34 (85.0)
Prior MI	10 (25.0)
Previous PCI	15 (37.5)
Previous CABG	1 (2.5)
Clinical presentation	
ST-segment elevation MI	4 (10.0)
Non ST-segment elevation MI	5 (12.5)
Unstable angina	5 (12.5)
Stable angina	26 (65.0)
Time to follow-up (days)	387.5 (317.8, 487.5)
Medication at follow-up	
Aspirin	36 (90.0)
Clopidogrel	38 (95.0)
Statin	37 (92.5)
β blocker	25 (62.5)
ACEI or ARB	25 (62.5)
Ca channel blocker	20 (50.0)
Laboratory data at follow-up	
Total cholesterol (mg/dl)	161.0 (134.8, 173.0)
LDL cholesterol (mg/dl)	88.0 (74.0, 98.8)
HDL cholesterol (mg/dl)	52.0 (40.0, 68.0)
Triglyceride (mg/dl)	122.0 (86.0, 168.0)
Hemoglobin A_{1C} (%)	6.2 (5.6, 7.1)
Estimated GFR (ml/min/1.73 m^2)	71.2 (62.3, 82.0)
Target vessel	
Left main	3 (7.5)
Left anterior descending artery	15 (37.5)
Left circumflex artery	10 (25.0)
Right coronary artery	15 (37.5)
Lesion type	
A or B1	18 (45.0)
B2 or C	22 (55.0)
Stent type	
Everolimus-eluting stent	36 (90.0)
Zotarolimus-eluting stent	2 (5.0)
Biolimus-eluting stent	2 (5.0)
De novo lesion	36 (90.0)
Number of stents (n)	1 (1, 2)
Minimum stent diameter (mm)	3.0 (2.8, 3.5)
Maximum stent diameter (mm)	3.25 (3.0, 3.5)
Total stent length (mm)	31.5 (23.0, 40.3)

Values are median (interquartile range) or n (%)

ACEI angiotensin-converting enzyme inhibitor, *ARB* angiotensin II receptor blocker, *CABG* coronary artery bypass graft surgery, *GFR* glomerular filtration ratio, *HDL* high-density lipoprotein, *LDL* low-density lipoprotein, *MI* myocardial infarction, *PCI* percutaneous coronary intervention

Table 2 Optical coherence tomography findings

Variable	Overall ($n=40$)
Patients with microchannels	13 (32.5)
Cross-sectional analysis	
Total cross sections analyzed (*n*)	1122
Mean stent CSA (mm^2)	8.2 (6.4, 10.1)
Mean lumen CSA (mm^2)	6.7 (5.2, 9.3)
Mean NIH CSA (mm^2)	1.1 (0.8, 1.4)
Percent NIH CSA (%)	13.2 (9.0, 16.8)
Uncovered struts (%)	12.7 (2.9, 40.8)
Malapposed struts (%)	0 (0, 5.2)
Microchannels (%)	3.0 (1.6, 7.2)
Strut-level analysis	
Total struts analyzed (*n*)	9974
Uncovered struts (%)	3.0 (0.6, 17.1)
Malapposed struts (%)	0 (0, 1.0)
Mean NIH thickness (μm)	112.1 (90.3, 153.0)

Values are median (interquartile range) or *n* (%). CSA: cross-sectional area

NIH neointimal hyperplasia

changes in OCT signal intensity of neointima tended to be higher in diabetic patients than in non-diabetic patients.

Several ultrasound studies have shown the enhancement of intraplaque microvessels in carotid arteries using intravenous microbubble administration [7, 8]. Previous studies have shown that microchannels defined as a no-signal tubuloluminal structure in coronary plaque identified by OCT are associated with plaque vulnerability [16]. On the other hand, from the pathological perspective, neoangiogenesis is closely associated with plaque progression and vulnerability and invisible microvessels even by OCT may be more important for intraplaque hemorrhage [1, 17, 18]. Virmani et al. showed that intraplaque microvessels were immature vessels with leaky structure and the primary source of intraplaque hemorrhage [17]. Another pathological study showed that the contents of necrotic core were derived from erythrocyte membrane, suggesting that the network of immature microvessels provided erythrocyte-derived phospholipids and free cholesterol [18]. These findings indicate that microvascular disruption or leakiness may promote lesion progression by providing erythrocyte-derived phospholipids and free cholesterol. Furthermore, Otsuka et al. demonstrated that hemorrhage within neoatherosclerotic plaque resulted from leaky microvessels [1]. In the present study, plaque enhancement by intracoronary microbubble administration indicates the possibility of neovascularization in neointima after drug-eluting stent implantation. Therefore, microbubble contrast-enhanced OCT imaging may be more useful to detect invisible microvessels and to identify vulnerable plaques. Moreover, our results suggest that microvessels within neointima should be a new target of pharmacological and interventional innovations for preventing stent failure. To the best of our knowledge, this is the first study to demonstrate the increase of OCT signal intensity in coronary vessel wall using microbubble contrast agents.

Diabetes mellitus is a major risk factor of cardiovascular events. Previous studies reported that utilizing OCT, microvessels were observed more frequently in in-stent restenotic tissue in diabetic patients and suggested that the formation of microvessels within in-stent restenosis may involve a unique pathophysiological factor in neoatherosclerosis in diabetic patients [6, 19]. It supports the results of the present study that showed a greater OCT intensity change of neointima after microbubble administration in diabetic patients compared to non-diabetic patients.

Pathological and clinical studies have shown that neoatherosclerosis after drug-eluting stents implantation

Table 3 Factors relative to greater intensity increase

Variable	Univariate analysis		Multivariate analysis	
	OR (95% CI)	*p* value	OR (95% CI)	*p* value
Age	0.993(0.933–1.058)	0.836	–	–
Male	1.714 (0.302–9.719)	0.543	–	–
Follow-up duration of OCT	0.997 (0.990–1.003)	0.394	–	–
Diabetes mellitus	10.000 (1.786–55.976)	0.009	10.000 (1.786–55.976)	0.009
Dyslipidemia	2.083 (0.215–20.170)	0.526	–	–
Statin use	0.741 (0.060–9.094)	0.815	–	–
Acute coronary syndrome	0.713 (0.154–3.297)	0.665	–	–
Chronic total occlusion lesion	2.800 (0.160–49.103)	0.481	–	–
Right coronary artery lesion	0.531(0.116–2.426)	0.414	–	–
De novo lesion	0.333 (0.041–2.722)	0.305	–	–
Minimum stent size	3.077 (0.461–20.531)	0.246	–	–
Stent length	0.983 (0.943–1.025)	0.423	–	–

OR odds ratio, *CI* confidence interval, *OCT* optical coherence tomography

Table 4 Patient and procedural characteristics in diabetic and non-diabetic patients

Variable	Diabetic ($n=18$)	Non-diabetic ($n=22$)	p value
Age (years)	64.5 (60.0, 74.0)	73.5 (64.0, 81.3)	0.10
Men	12 (66.7)	18 (81.8)	0.23
Body Mass Index (kg/m^2)	23.4 (22.2, 25.0)	22.7 (21.2, 25.6)	0.42
Current smoker	4 (22.2)	2 (9.1)	0.24
Hypertension	15 (83.3)	16 (72.7)	0.34
Dyslipidemia	17 (94.4)	17 (77.3)	0.14
Prior MI	5 (27.8)	5 (22.7)	0.50
Previous PCI	7 (38.9)	8 (36.4)	0.56
Previous CABG	0	1 (4.5)	0.55
Clinical presentation			
ST-segment elevation MI	2 (11.1)	2 (9.1)	0.62
Non ST-segment elevation MI	2 (11.1)	3 (13.6)	0.60
Unstable angina	1 (5.6)	4 (18.2)	0.24
Stable angina	13 (72.2)	13 (59.1)	0.39
Time to follow-up (days)	428.0 (314.0, 493.5)	378.5 (324.3, 486.0)	0.80
Medication at follow-up			
Aspirin	16 (88.9)	20 (90.9)	0.62
Clopidogrel	17 (94.4)	21 (95.5)	0.70
Statin	17 (94.4)	20 (90.9)	0.58
β blocker	10 (55.6)	15 (68.2)	0.41
ACEI or ARB	11 (61.1)	14 (63.6)	0.87
Ca channel blocker	9 (50.0)	11 (50.0)	1.00
Laboratory data at follow-up			
Total cholesterol (mg/dl)	162.0 (149.0, 171.0)	154.0 (130.5, 175.0)	0.71
LDL cholesterol (mg/dl)	91.0 (74.0, 100.0)	88.0 (72.3, 99.0)	0.62
HDL cholesterol (mg/dl)	53.0 (40.0, 77.5)	52.0 (40.0, 68.0)	0.74
Triglyceride (mg/dl)	141.0 (97.5, 183.5)	121.0 (81.5, 146.8)	0.17
Hemoglobin A_{1C} (%)	7.1 (6.7, 7.8)	5.6 (5.4, 5.9)	<0.001
Estimated GFR (ml/min/1.73 m^2)	72.1 (62.2, 84.7)	70.1 (61.8, 82.5)	0.80
Target vessel			
Left main	1 (5.6)	2 (9.1)	0.58
Left anterior descending artery	8 (44.4)	7 (31.8)	0.41
Left circumflex artery	4 (22.2)	6 (27.3)	0.50
Right coronary artery	6 (33.3)	9 (40.9)	0.62
Lesion type			
A or B1	9 (50.0)	9 (40.9)	0.57
B2 or C	9 (50.0)	13 (59.1)	0.57
Stent type			
Everolimus-eluting stent	15 (83.3)	21 (95.5)	0.23
Zotarolimus-eluting stent	1 (5.6)	1 (4.5)	0.70
Biolimus-eluting stent	2 (11.1)	0	0.20
De novo lesion	16 (88.9)	20 (90.9)	0.62
Number of stents (n)	1 (1, 2)	1 (1, 2)	0.88
Minimum stent diameter (mm)	3.0 (2.9, 3.5)	3.0 (2.7, 3.5)	0.94
Maximum stent diameter (mm)	3.0 (3.0, 3.5)	3.5 (3.0, 3.5)	0.50
Total stent length (mm)	33.0 (27.5, 42.5)	25.5 (21.8, 43.5)	0.41

Values are median (interquartile range) or n (%)

ACEI angiotensin-converting enzyme inhibitor, *ARB* angiotensin II receptor blocker, *CABG* coronary artery bypass graft surgery, *GFR* glomerular filtration ratio, *HDL* high-density lipoprotein, *LDL* low-density lipoprotein, *MI* myocardial infarction, *PCI* percutaneous coronary intervention

Table 5 Optical coherence tomography findings in diabetic and non-diabetic patients

Variable	Diabetic ($n=18$)	Non-diabetic ($n=22$)	p value
Patients with microchannels	6 (33.3)	7 (31.8)	0.92
Cross-sectional analysis			
Total cross sections analyzed (n)	538	584	
Mean stent CSA (mm^2)	8.1 (6.4, 11.6)	8.2 (6.7, 9.6)	0.96
Mean lumen CSA (mm^2)	6.9 (5.7, 10.2)	6.7 (4.8, 8.7)	0.43
Mean NIH CSA (mm^2)	1.0 (0.8, 1.2)	1.1 (0.8, 1.7)	0.36
Percent NIH CSA (%)	11.4 (8.4, 16.3)	14.3 (11.0, 20.5)	0.33
Uncovered struts (%)	25.1 (9.1, 52.0)	8.7 (0, 30.8)	0.07
Malapposed struts (%)	3.0 (0, 12.7)	0 (0, 0.9)	0.04
Microchannels (%)	2.7 (1.5, 8.5)	3.3 (1.4, 9.6)	0.67
Strut-level analysis			
Total struts analyzed (n)	4645	5329	
Uncovered struts (%)	9.2 (1.4, 25.0)	1.5 (0, 5.2)	0.02
Malapposed struts (%)	0.4 (0, 2.5)	0 (0, 1.2)	0.049
Mean NIH thickness (μm)	103.9 (74.2, 135.2)	125.4 (99.7, 165.3)	0.17

Values are median (interquartile range) or n (%)

CSA cross-sectional area, *NIH* neointimal hyperplasia

is observed earlier compared to bare metal stents. The development of neoatherosclerosis occurs in months to years following drug-eluting stent implantation, whereas atherosclerosis in native coronary arteries develops over decades [1]. In the present study, neovascularization in the early phase after drug-eluting stent implantation may have been identified, because follow-up OCT was performed at a median time of 387.5 days.

Vulnerable neoatherosclerosis may cause late stent thrombosis. Further studies are required whether neointima enhanced by intracoronary microbubble administration causes cardiovascular events during follow-up.

Limitations

This study had several limitations. First, the number of enrolled patients was relatively small. Secondly, the optimal time interval from stent implantation to follow-up OCT is unknown. Microvessels within in-stent neoatherosclerosis have been reported to increase with time. The present study showed that the median of %NIH CSA was 13.2%. However the rate was not much different from results in recent studies [13, 20, 21], the degree of neointima might not be enough to be analyzed. Third, the position of the imaging catheter used to estimate OCT signal intensity of neointima should be uniform in all cases. The degree of neointimal OCT signal intensity could be affected by the position of the imaging catheter in the lumen. Lastly, pathological validation of neovascularization in neointima was not performed.

Conclusions

Intracoronary administration of microbubble contrast agents enhanced OCT signal intensity of neointima in patients treated with drug-eluting stents. The present study suggested that microbubble contrast enhancement in OCT imaging may be useful to identify neovascularization in neointima and evaluate vulnerability of neoatherosclerosis. Microvessels in neointima may be a future target of pharmacological and interventional innovations for preventing stent failure.

Compliance with ethical standards

Conflict of interest The authors declare that they have no conflict of interest.

Ethical approval All procedures performed in studies involving human participants were in accordance with the ethical standards of the institutional and/or national research committee and with the 1964 Helsinki declaration and its later amendments or comparable ethical standards.

References

1. Otsuka F, Byrne RA, Yahagi K, Mori H, Ladich E, Fowler DR, Kutys R, Xhepa E, Kastrati A, Virmani R, Joner M (2015) Neoatherosclerosis: overview of histopathologic findings and implications for intravascular imaging assessment. Eur Heart J 36:2147–2159
2. Nakazawa G, Otsuka F, Nakano M, Vorpahl M, Yazdani SK, Ladich E, Kolodgie FD, Finn AV, Virmani R (2011) The

pathology of neoatherosclerosis in human coronary implants bare-metal and drug-eluting stents. J Am Coll Cardiol 57:1314–1322
3. Nakazawa G, Vorpahl M, Finn AV, Narula J, Virmani R (2009) One step forward and two steps back with drug-eluting-stents: from preventing restenosis to causing late thrombosis and nouveau atherosclerosis. JACC Cardiovasc Imaging 2:625–628
4. Habara M, Terashima M, Nasu K, Kaneda H, Yokota D, Ito T, Kurita T, Teramoto T, Kimura M, Kinoshita Y, Tsuchikane E, Asakura Y, Suzuki T (2013) Morphological differences of tissue characteristics between early, late, and very late restenosis lesions after first generation drug-eluting stent implantation: an optical coherence tomography study. Eur Heart J Cardiovasc Imaging 14:276–284
5. Taruya A, Tanaka A, Nishiguchi T, Matsuo Y, Ozaki Y, Kashiwagi M, Shiono Y, Orii M, Yamano T, Ino Y, Hirata K, Kubo T, Akasaka T (2015) Vasa vasorum restructuring in human atherosclerotic plaque vulnerability: a clinical optical coherence tomography study. J Am Coll Cardiol 65:2469–2477
6. Suzuki N, Kozuma K, Kyono H, Otsuki S, Fu Q, Hosogoe N, Saito T, Naito K, Ochiai M, Ishikawa S, Watanabe H, Miyazawa A, Eto K, Isshiki T (2013) Predominant microvessel proliferation in coronary stent restenotic tissue in patients with diabetes: insights from optical coherence tomography image analysis. Int J Cardiol 168:843–847
7. Saito K, Nagatsuka K, Ishibashi-Ueda H, Watanabe A, Kannki H, Iihara K (2014) Contrast-enhanced ultrasound for the evaluation of neovascularization in atherosclerotic carotid artery plaques. Stroke 45:3073–3075
8. Staub D, Patel MB, Tibrewala A, Ludden D, Johnson M, Espinosa P, Coll B, Jaeger KA, Feinstein SB (2010) Vasa vasorum and plaque neovascularization on contrast-enhanced carotid ultrasound imaging correlates with cardiovascular disease and past cardiovascular events. Stroke 41:41–47
9. Assadi H, Demidov V, Karshafian R, Douplik A, Vitkin IA (2016) Microvascular contrast enhancement in optical coherence tomography using microbubbles. J Biomed Opt 21:76014–76018
10. Barton JK, Hoying JB, Sullivan CJ (2002) Use of microbubbles as an optical coherence tomography contrast agent. Acad Radiol 9(Suppl 1):S52–S55
11. Assadi H, Karshafian R, Douplik A (2014) Optical scattering properties of intralipid phantom in presence of encapsulated microbubbles. Int J Photoenergy 2014:1–9
12. Kadohira T, Kobayashi Y (2017) Intravascular ultrasound-guided drug-eluting stent implantation. Cardiovasc Interv Ther 32:1–11
13. Kim JS, Hong MK, Shin DH, Kim BK, Ko YG, Choi D, Jang Y (2012) Quantitative and qualitative changes in DES-related neointimal tissue based on serial OCT. JACC Cardiovasc Imaging 5:1147–1155. https://doi.org/10.1016/j.jcmg.2012.01.024
14. Tearney GJ, Regar E, Akasaka T, Adriaenssens T, Barlis P, Bezerra HG, Bouma B, Bruining N, Cho JM, Chowdhary S, Costa MA, De Silva R, Dijkstra J, Di Mario C, Dudeck D, Falk E, Feldman MD, Fitzgerald P, Garcia H, Gonzalo N, Granada JF, Guagliumi G, Holm NR, Honda Y, Ikeno F, Kawasaki M, Kochman J, Koltowski L, Kubo T, Kume T, Kyono H, Lam CCS, Lamouche G, Lee DP, Leon MB, Maehara A, Manfrini O, Mintz GS, Mizuno K, Morel MA, Nadkarni S, Okura H, Otake H, Pietrasik A, Prati F, Rber L, Radu MD, Rieber J, Riga M, Rollins A, Rosenberg M, Sirbu V, Serruys PWJC, Shimada K, Shinke T, Shite J, Siegel E, Sonada S, Suter M, Takarada S, Tanaka A, Terashima M, Troels T, Uemura S, Ughi GJ, Van Beusekom HMM, Van Der Steen AFW, Van Es GA, Van Soest G, Virmani R, Waxman S, Weissman NJ, Weisz G (2012) Consensus standards for acquisition, measurement, and reporting of intravascular optical coherence tomography studies: a report from the International Working Group for Intravascular Optical Coherence Tomography Standardization and Validation. J Am Coll Cardiol 59:1058–1072. https://doi.org/10.1016/j.jacc.2011.09.079
15. Di Vito L, Yoon JH, Kato K, Yonetsu T, Vergallo R, Costa M, Bezerra HG, Arbustini E, Narula J, Crea F, Prati F, Jang I-K, COICO Group (Consortium of Investigators for Coronary OCT) (2014) Comprehensive overview of definitions for optical coherence tomography-based plaque and stent analyses. Coron Artery Dis 25:172–185
16. Kitabata H, Tanaka A, Kubo T, Takarada S, Kashiwagi M, Tsujioka H, Ikejima H, Kuroi A, Kataiwa H, Ishibashi K, Komukai K, Tanimoto T, Ino Y, Hirata K, Nakamura N, Mizukoshi M, Imanishi T, Akasaka T (2010) Relation of microchannel structure identified by optical coherence tomography to plaque vulnerability in patients with coronary artery disease. Am J Cardiol 105:1673–1678
17. Virmani R, Kolodgie FD, Burke AP, Finn AV, Gold HK, Tulenko TN, Wrenn SP, Narula J (2005) Atherosclerotic plaque progression and vulnerability to rupture: angiogenesis as a source of intraplaque hemorrhage. Arterioscler Thromb Vasc Biol 25:2054–2061
18. Kolodgie FD, Gold HK, Burke AP, Fowler DR, Kruth HS, Weber DK, Farb A, Guerrero LJ, Hayase M, Kutys R, Narula J, Finn AV, Virmani R (2003) Intraplaque hemorrhage and progression of coronary atheroma. N Engl J Med 349:2316–2325
19. Gao L, Park S-J, Jang Y, Lee S, Kim C-J, Minami Y, Ong D, Soeda T, Vergallo R, Lee H, Yu B, Uemura S, Jang I-K (2015) Comparison of neoatherosclerosis and neovascularization between patients with and without diabetes: an optical coherence tomography study. JACC Cardiovasc Interv 8:1044–1052
20. Nakamura D, Lee Y, Yoshimura T, Taniike M, Makino N, Kato H, Egami Y, Shutta R, Tanouchi J, Yamada Y, Hara M, Sakata Y, Hamasaki T, Nishino M (2014) Different serial changes in the neointimal condition of sirolimus-eluting stents and paclitaxel-eluting stents: an optical coherence tomographic study. EuroIntervention 10:924–933. https://doi.org/10.4244/EIJV10I8A159
21. Kubo T, Akasaka T, Tanimoto T, Takano M, Seino Y, Nasu K, Itoh T, Mizuno K, Okura H, Shinke T, Kotani JI, Ito S, Yokoi H, Muramatsu T, Nakamura M, Nanto S (2016) Assessment of vascular response after drug-eluting stents implantation in patients with diabetes mellitus: an optical coherence tomography substudy of the J-DESsERT. Heart Vessels 31:465–473. https://doi.org/10.1007/s00380-015-0636-6